NACA

RESEARCH MEMORANDUM

INFLUENCE OF COMBUSTION-CHAMBER LENGTH ON AFTERBURNER PERFORMANCE

By James W. Useller, Willis M. Braithwaite, and Carl J. Rudey

Lewis Flight Propulsion Laboratory
Cleveland, Ohio

NATIONAL ADVISORY COMMITTEE
FOR AERONAUTICS

WASHINGTON

August 27, 1954

NACA RM E54E06

NATIONAL ADVISORY COMMITTEE FOR AERONAUTICS

RESEARCH MEMORANDUM

INFLUENCE OF COMBUSTION-CHAMBER LENGTH ON AFTERBURNER PERFORMANCE

By James W. Useller, Willis M. Braithwaite, and Carl J. Rudey

SUMMARY

The influence of combustion-chamber length on afterburner performance was investigated under conditions simulating altitude flight. The component design and arrangement were selected from the results of previous investigations to produce maximum thrust augmentation near the stoichiometric condition. The combustion-chamber length was varied in progressive increments from 3 to $6\frac{1}{2}$ feet. The combustion efficiency, combustion temperature, and augmented jet-thrust ratio increased rapidly with combustion-chamber length up to 5 feet, after which further increases in combustion-chamber length produced only small increases in performance. Reducing the afterburner-inlet pressure did not change the afterburner performance trends with length. Afterburners with combustion-chamber lengths of 4 feet or less required only a small flow of external cooling air to maintain safe structural temperatures. Increasing the combustion-chamber length increased the cooling-air flow required. For the particular configuration investigated, the most favorable afterburner combustion-chamber lenght, considering both performance and cooling requirements, was about 5 feet. This length was not significantly changed by the afterburner equivalence ratio or flight condition.

INTRODUCTION

A series of investigations aimed at the improvement of the design and the performance of turbojet-engine afterburners has been undertaken at the NACA Lewis laboratory. Included in these investigations were studies of the effects of the diffuser design (refs. 1 and 2, e.g.), the fuel spray characteristics (ref. 3), the flame-holder design (ref. 4), and the afterburner-inlet velocity (ref. 5) on the ability of the afterburner to efficiently augment the performance of a turbojet engine. The high gas temperatures associated with maximum performance have also prompted investigations of methods to adequately cool the afterburner structure (refs. 6 and 7). In addition to these variables, the time available for fuel mixing, vaporization, and combustion (commonly called resident time) will influence the afterburner performance. Because the afterburner diameter is usually determined by the space limitation of the air-frame installation, the resident time usually can only be controlled by changing the length of the afterburner combustion chamber.

Determination of the effect of the combustion-chamber length on the performance and cooling requirements of the afterburner was the objective of the investigation reported herein.

An afterburner designed to operate at a high performance level was constructed in such a manner that the combustion-chamber length could be varied from 3 to $6\frac{1}{2}$ feet in progressive increments. The effect of varying the combustion-chamber length on the combustion efficiency and temperature was investigated at afterburner-inlet pressures of 1050 and 1600 pounds per square foot absolute (simulated flight at a Mach number of 1.0 and an altitude of 35,000 ft and for a flight Mach number of 0.8 and an altitude of 40,000 ft). The effect of combustion-chamber length on the altitude operating limits and on the afterburner-structure cooling requirements was also determined.

APPARATUS AND INSTRUMENTATION

Engine. - The axial-flow turbojet engine used in this investigation developed 3000 pounds of thrust at sea-level conditions with an engine air flow of 58 pounds per second, an average turbine-outlet gas temperature of 1625° R, and a rated engine speed of 12,500 rpm. The fuel used in the primary engine combustor was clear, unleaded gasoline (62-octane).

Afterburner. - A schematic diagram of the afterburner assembly is shown in figure 1. The primary components of the afterburner included a conical annular diffuser, a two-ring V-gutter flame holder with an area blockage of 34.7 percent, a fixed-area exhaust nozzle, and an external manifold fuel system. The combustion-chamber lengths investigated and the corresponding fixed-area exhaust nozzle used are shown in the table accompanying figure 1. The afterburner was designed to provide a gas velocity at the leading edge of the flame holder of approximately 530 feet per second. Vortex generators were welded to the upstream end of the conical-diffuser inner cone to prevent flow separation. The afterburner combustion chamber had a constant diameter of 22.8 inches and was air cooled from a point immediately downstream of the flame holder to the exhaust-nozzle outlet. Afterburner cooling air was supplied at room temperature from an outside source.

The afterburner fuel was introduced through a series of 24 radial fuel spray bars that were equally spaced around the circumference of the afterburner and were located approximately 25 inches upstream of the flame holder. Twelve of the spray bars had eight holes and the alternate twelve bars had only six holes. The diameter and spacing of the spray-bar holes (shown in fig. 2) were such as to provide a uniform fuel-air profile across the afterburner diameter, as recommended in reference 3 for good performance. A mass-flow profile was determined as the basis for the design of the fuel-spray system and is shown in figure 3(a). The fuel spray bars were designed to provide fuel flow matched to the air flow

pattern during stoichiometric operation with the resultant radial fuel-air ratio pattern shown in figure 3(b). The fuel-air ratio was reduced slightly near the afterburner wall for all configurations investigated to reduce the maximum wall temperature. Afterburner ignition was accomplished by means of a hot streak initiated by a stream of additional fuel being injected at the turbine inlet. The afterburner fuel was MIL-F-5624A grade JP-4.

Instrumentation. - The engine air flow was measured by means of a venturi section ahead of the engine inlet by the use of the static pressures in the venturi throat and the total pressure of the altitude-chamber inlet. The afterburner cooling-air flow was measured by an A.S.M.E. designed orifice. The engine and afterburner fuel flows were measured by calibrated rotameters. An NACA gas mixture analyzer was used to sample the afterburner fuel-air ratio at various positions in the afterburner. A description of the analyzer and the sampling technique employed is contained in reference 3.

The instrumentation installed in the engine and afterburner is shown in the following table:

	Station			
	1 (Engine inlet)	5 (Turbine outlet)	9 (Exhaust-nozzle inlet)	10 (Exhaust-nozzle outlet)
Total-temperature thermocouples	20	48	--	--
Total-pressure probes	(a)	20	13	--
Static-pressure probes	6 (wall)	4 (wall)	--	8 (lip)[b]

[a]Engine-inlet total pressure was assumed equal to altitude-chamber inlet pressure.

[b]Four lip static-pressure probes were mounted 90° apart on both the primary and the secondary nozzles as shown in figure 1.

As part of the afterburner cooling phase of this study, four skin thermocouples were spot-welded 90° apart on the afterburner wall at each of the following stations, as measured downstream from the flame holder:

Nominal combustion-chamber length, ft	Thermocouple location, in. from flame holder
6.5	16, 60, 70.56, 73.56, 76.56
5.0	16, 44, 52.56, 55.56, 58.56
4.0	16, 32, 40.56, 43.56, 46.56
3.0	16, 20, 28.56, 31.56, 34.56

3272

The combustion-chamber length is hereinafter defined as the distance between the flame holder and the exhaust-nozzle outlet.

Installation. - The turbojet-engine afterburner configuration was installed in an altitude test chamber which permitted simulation of engine-inlet temperatures and pressures corresponding to the desired flight conditions and exhaust pressures corresponding to the altitude being simulated. The engine was mounted on a suspended thrust bed which was connected through a null-type thrust measuring cell to the altitude chamber.

PROCEDURE

The afterburner combustion-chamber length was varied by inserting or removing cylindrical sections of the afterburner and cooling shroud between the flame-holder location and the exhaust-nozzle inlet. Combustion-chamber lengths of $6\frac{1}{2}$, 5, 4, and 3 feet were investigated.

For each afterburner combustion-chamber length investigated, performance data were obtained at nominal afterburner-inlet pressures of 1600 and 1050 pounds per square foot over a range of equivalence ratios (fraction of stoichiometric fuel-air ratio) from lean blow-out to stoichiometric or until the limiting turbine-outlet gas temperature was reached (1625° R).

For each combustion-chamber length, the altitude operational limit was determined for a flight Mach number of 0.8 by increasing the altitude in 1000-foot increments until blow-out occurred or a stoichiometric condition was reached.

The cooling-air flow requirements of the afterburner were studied by varying the air flow from 5 to 35 percent of the afterburner gas flow. A limiting wall temperature was established by maintaining a maximum individual wall temperature of 2000° R. The afterburner cooling studies

were conducted with the afterburner operating at a stoichiometric fuel-air ratio. The symbols used throughout this report are defined in appendix A, and the methods of calculation are given in appendix B.

RESULTS AND DISCUSSION

The performance level and the operational limits of turbojet-engine afterburners are affected by the interaction of the performance characteristics of the afterburner components. In order to eliminate the influence of all components other than combustion-chamber length, all other variables were fixed as much as was feasible throughout the investigation.

Afterburner-inlet conditions. - The use of a fixed-area exhaust nozzle and the variation of total-pressure loss with length precluded the establishment of exactly similar afterburner-inlet conditions of temperature, total pressure, and velocity. The variation of these parameters with combustion-chamber length is shown in figure 4 for several afterburner equivalence ratios and for two flight conditions during stoichiometric afterburning. An increase in the afterburner-inlet average temperature of approximately 15 percent (200° to 250° R) was measured for a variation of combustion-chamber length from 3 to $6\frac{1}{2}$ feet (fig. 4(a)). A change of approximately 9 percent was effected in the inlet temperature when the equivalence ratio was varied from 0.7 to 1.0. The afterburner-inlet total pressure (fig. 4(b)) increased similarly with increasing combustion-chamber length. The afterburner-inlet average gas velocity decreased approximately 40 feet per second with the extension of the combustion-chamber length (fig. 4(c)). Although qualitative comparisons of the afterburner performance are possible, the variation of the afterburner-inlet flow conditions with combustion-chamber length tends to penalize the shorter afterburners and must be considered in the final evaluation of the performance.

The effect of varying the combustion-chamber length on the combustion efficiency and temperature is shown in figures 5(a) and (b), respectively, for several equivalence ratios during simulated flight at a Mach number of 1.0 and an altitude of 35,000 feet. As might be anticipated, both combustion efficiency and combustion temperature are relatively low for the short afterburners (combustion-chamber lengths from 3 to 4 ft) due to insufficient resident time. The combustion performance increases rapidly with combustion-chamber length until a maximum is reached for lengths between 5 and $6\frac{1}{2}$ feet. The actual length at which maximum combustion performance is reached is a function of the equivalence ratio, with longer combustion chambers being required at lower equivalence ratios.

[redacted]

The augmented jet-thrust ratios resulting from the combustion performance are shown in figure 5(c). The thrust augmentation also increases rapidly from a relatively low value at a length of 3 feet to a maximum at a length slightly greater than 5 feet. Further increases in length and consequently in fuel resident time fail to produce additional increases in thrust augmentation because of the continuing increase in total-pressure loss with length. The increase of the total-pressure loss parameter with the combustion-chamber length is shown in figure 5(d).

The total-pressure loss parameter followed a trend similar to that of the augmented jet-thrust ratio with varying combustion-chamber length except that a maximum was not reached. The pressure loss increased rapidly for afterburner lengths up to approximately 5 feet and exhibited only small increases in the pressure loss parameter for lengths in excess of 5 feet. The total-pressure loss in the afterburner is shown as a function of the impact pressure $(P_5 - p_5)$ in order to minimize the effect of afterburner-inlet velocity changes.

The variation in afterburner performance associated with a change in afterburner-inlet total pressure is shown in figure 6. For an equivalence ratio of 1.00 (stoichiometric fuel-air ratio), decreasing the afterburner-inlet total pressure from 1600 to 1050 pounds per square foot absolute (fig. 6(a)) decreased the combustion efficiency 0.12 and 0.07 for combustion-chamber lengths of 4 and 6 feet, respectively. Accompanying this decrease in combustion efficiency was a reduction in combustion temperature (fig. 6(b)) between 200° and 350° R and a decrease in the augmented jet-thrust ratio (fig. 6(c)) between 0.15 and 0.10, with the smaller thrust loss being associated with the longer combustion chamber. The total-pressure loss parameter (fig. 6(d)) was approximately 0.02 higher at the lower afterburner-inlet pressure than at the higher pressure.

Changing the afterburner-inlet pressure from 1600 to 1050 pounds per square foot absolute reduced the performance of the afterburner but did not change the performance trends with increase in combustion-chamber length.

Operational limits. - The afterburner was operated with each of the combustion-chamber lengths at a flight Mach number of 0.8 and equivalence ratios from 0.8 to 0.9 to determine the maximum operable altitude. The shortest afterburner (3-foot combustion chamber) was operable to a maximum altitude of 45,200 feet, while the afterburner with a combustion-chamber length of $6\frac{1}{2}$ feet was operable to an altitude of 47,600 feet (fig. 7). In considering the maximum operable altitudes encountered with this afterburner, it must be remembered that the achievement of maximum thrust augmentation with an afterburner usually requires a compromise of the altitude and lean operational characteristics. An afterburner capable of high augmentation performance will require a fuel distribution system that will not necessarily be ideal for lean operation

and vice versa. Although the curve of maximum altitude operation limit shown in figure 7 appears to continue to increase with combustion-chamber length, the rate of increase is small. There would obviously be a length beyond which the altitude limit would not increase further. The small increase in the altitude limit is attributed to the slightly higher afterburner-inlet pressure level associated with increasing afterburner length.

The effect of the combustion-chamber length on the equivalence ratio at which lean combustion blow-out occurred is shown in figure 8 for two flight conditions. In general, the increased residence time permitted operation at leaner fuel-air ratios (lower equivalence ratios). During operation at an afterburner-inlet pressure of 1600 pounds per square foot absolute, the lean blow-out operational limit decreased from an equivalence ratio of 0.63 for the 3-foot combustion chamber to 0.50 when the $6\frac{1}{2}$-foot combustion chamber was investigated. A similar trend is shown for operation at an afterburner-inlet pressure of 1050 pounds per square foot absolute. Some increase in the lean operation may be attributed to the increased pressure level in the afterburner with increased length, although the pressure effect on the lean operational limit is shown to be small in figure 8.

Structural cooling requirements. - Operation of conventional afterburners at high temperatures and high efficiencies requires a considerable quantity of cooling air to maintain the structural temperatures within safe limits. Although the average wall temperature is important for installation purposes, local individual temperatures will determine structural failures due to overheating. The maximum individual afterburner wall temperatures measured during the investigation are shown in figure 9 for cooling-air flow from zero to 35 percent of the afterburner gas flow. A maximum local temperature of 2000° R was used as the limit for safe operation during this investigation. Combustion-chamber lengths of less than 4 feet do not require auxiliary cooling air to maintain temperatures below 1550° R. This is a result of the provision in this particular fuel-system design for lean fuel-air ratios adjacent to the afterburner structure. Combustion chambers greater than 4 feet in length require sizeable quantities of cooling air to maintain safe maximum structure temperatures. For example, a 5-foot-long combustion chamber would require a cooling-air flow of 10 percent of the afterburner gas flow for a maximum structure temperature of 1915° R, 15 percent weight flow for a maximum temperature of 1750° R, and proportionately larger quantities of cooling-air flow to maintain lower maximum structure temperatures. Any further increase in the combustion-chamber length would require even greater quantities of cooling-air flow to maintain a given structure temperature.

CONCLUDING REMARKS

The effect of combustion-chamber length on combustion efficiency, cooling requirements, and operational limits was investigated on an afterburner designed to operate at a high performance level. The combustion efficiency, combustion temperature, and augmented jet-thrust ratio increased rapidly with combustion-chamber length up to approximately 5 feet. Further increases in the combustion-chamber length produced only small increases in performance. The total-pressure loss in the afterburner followed a similar trend with only small increases in the pressure loss parameter for lengths in excess of 5 feet. Changing the afterburner-inlet pressure from 1600 pounds per square foot (associated with a flight condition simulating a Mach number of 1.0 and an altitude of 35,000 ft) to 1050 pounds per square foot (flight Mach number of 0.8 and altitude of 40,000 ft) reduced the performance of the afterburner but did not change the performance trends with increase in combustion-chamber length. The effect of the combustion-chamber length on the maximum operable altitude and on the limit of lean operation was slight for the range of flight conditions investigated. For the configuration investigated, as the combustion-chamber length was increased beyond 4 feet, substantial increases in cooling-air flow were required in order to maintain a given afterburner wall temperature.

The afterburner performance, the normal losses in the afterburner, and the structural cooling requirements indicate that the most desirable combustion-chamber length for an afterburner of the type investigated is approximately 5 feet and that this length is not significantly influenced by the afterburner equivalence ratio or flight condition.

Lewis Flight Propulsion Laboratory
National Advisory Committee for Aeronautics
Cleveland, Ohio, May 14, 1954

APPENDIX A

SYMBOLS

The following symbols are used in this report:

A	cross-sectional area, sq ft
C_d	coefficient of discharge, ratio of measured to theoretical mass flow through exhaust nozzle
C_v	velocity coefficient, ratio of actual effective jet velocity to theoretical effective jet velocity
F_j	jet thrust, lb
F_j'	calculated nonafterburning jet thrust, lb
f	fuel-air ratio
g	acceleration due to gravity, 32.2 ft/sec^2
h	enthalpy, Btu/lb
L	combustion-chamber length, ft
M	Mach number
m	mass flow
P	total pressure, lb/sq ft abs
p	static pressure, lb/sq ft abs
R	gas constant, $\frac{1546 \text{ ft-lb}}{(\text{molecular weight})(\text{lb})(^\circ\text{R})}$
T	total temperature, $^\circ$R
V	velocity, ft/sec
W_a	air flow, lb/sec
W_f	fuel flow, lb/hr
W_g	gas flow, lb/sec

γ	ratio of specific heats
η	combustion efficiency
φ	equivalence ratio (fraction of stoichiometric fuel-air ratio)

Subscripts:

a	air
b	afterburner
c	cooling air
e	engine
i	ideal
0	free-stream conditions
1	engine inlet
5	turbine outlet
6	flame holder (afterburner combustion-chamber inlet)
9	exhaust-nozzle inlet
10	exhaust-nozzle outlet

APPENDIX B

METHODS OF CALCULATIONS

Flight Mach number. - The simulated flight Mach number was calculated from the following relation with complete ram recovery at the engine inlet assumed:

$$M_O = \sqrt{\frac{2}{\gamma_1 - 1}\left[\left(\frac{P_1}{P_O}\right)^{\frac{\gamma_1 - 1}{\gamma_1}} - 1\right]} \tag{1}$$

where γ for the inlet air was assumed to be 1.4 and P_1 was measured in the altitude-chamber inlet section.

Air flow. - The engine air flow was calculated from pressure and temperature measurements obtained in the engine-inlet duct by the following equation:

$$W_{a,1} = A_1 P_1 \sqrt{\frac{2\gamma g}{(\gamma - 1)RT_1}\left[\left(\frac{P_1}{p_1}\right)^{\frac{\gamma - 1}{\gamma}} - 1\right]} \tag{2}$$

The gas flow at the exit of the afterburner was then computed as

$$W_g = W_{a,1} + \frac{W_{f,e} + W_{f,b}}{3600} \tag{3}$$

Equivalence ratio. - The engine equivalence ratio was computed as

$$\varphi_e = 14.99 \frac{W_{f,e}}{3600 W_{a,1}} \tag{4}$$

The afterburner equivalence ratio was computed on the basis of the afterburner fuel flow and the unburned air and fuel entering the afterburner:

$$\varphi_b = \frac{14.82}{3600}\left[\frac{W_{f,b}}{W_{a,1}} + \frac{14.99}{14.82}\left(\frac{W_{f,e} - W_{f,e,i}}{W_{a,1}}\right)\right]\frac{W_{a,1}}{W_{a,1}(1 - \varphi_{e,i})} \tag{5}$$

[redacted]

where 14.99 is the stoichiometric air-fuel ratio for the engine fuel, 14.82 is the stoichiometric air-fuel ratio for the afterburner fuel, and

$$W_{f,e,i} = W_{a,1}\left[\frac{\Delta h_a\Big]_1^5}{h_{c,e} - \lambda_{5,e}}\right]$$

$$\varphi_{e,i} = 14.99\,\frac{W_{f,e,i}}{W_{a,1}} \tag{6}$$

where λ is the difference between the enthalpy of the oxygen of the incoming air and the enthalpy of carbon dioxide and water vapor formed by combustion (ref. 7), and $W_{f,e,i}$ is the fuel flow required for the enthalpy rise across the combustor with 100-percent combustion efficiency.

Augmented jet-thrust ratio. - The augmented jet-thrust ratio is defined as the ratio of the jet thrust of the afterburning engine to the jet thrust of the engine equipped with a nonafterburning tail pipe and operating at the same turbine-outlet total temperature and pressure. The jet thrust of the afterburning engine was obtained from the equation

$$F_j = F_{scale} + (A\Delta p)_{seal} - F_c \tag{7}$$

where F_{scale} is the thrust scale reading, $(A\Delta p)_{seal}$ is the area of the engine at the labyrinth seal in the front bulkhead of the altitude test chamber multiplied by the pressure difference across this bulkhead, and F_c is the thrust due to the cooling-air flow as determined by pressure and temperature measurements in the cooling passage.

The nonafterburning jet thrust F_j' was computed with the assumption of a 3-percent total-pressure loss between the turbine outlet and the exhaust nozzle of the nonburning tail pipe:

$$F_j' = \left(W_{a,1} + \frac{W_{f,e}}{3600}\right)\left(\frac{V_e}{\sqrt{gRT}}\right)_9 \frac{\sqrt{gRT_9}}{g}\,C_v \tag{8}$$

where $T_9 = T_5$; $\left(\frac{V_e}{\sqrt{gRT}}\right)_9$ is the effective velocity parameter as defined in reference 8 and is a function of γ_5 and $\frac{P_{10}}{P_9}$; $P_9 = 0.97P_5$; and $C_v = 0.99$.

Exhaust-gas total temperature. - In order to compute the afterburning exhaust-gas total temperature, it was necessary first to compute the exhaust-nozzle total pressure. This was determined from the following relation, which was derived in reference 9 for a choked nozzle:

$$\frac{F_j}{C_v C_d A_{10}} = (\gamma + 1)\left(\frac{2}{\gamma + 1}\right)^{\frac{\gamma}{\gamma-1}} P_{10} - p_0 \qquad (10)$$

where the values of C_d are a function of P_{10}/p_0 and were obtained from reference 10, and C_v is 0.99 as previously defined.

The exhaust-gas total temperature was then computed from the equation:

$$T_{10} = \frac{g}{R}\left[\left(\frac{W\sqrt{(R/g)T}}{PA}\right)_{10}\left(\frac{P_{10}A_{10}C_d}{W_g}\right)\right]^2 \qquad (11)$$

where $\left(\frac{W\sqrt{(R/g)T}}{PA}\right)_{10}$ is the total-pressure parameter for critical flow at the exhaust-nozzle exit as derived in reference 8.

Afterburner-inlet velocity. - The velocity at the afterburner inlet was computed from a static-pressure measurement, the total temperature, the weight flow, and the area at station 6 by using the one-dimensional flow parameters of reference 8:

$$V_6 = \left(\frac{V}{\sqrt{gRT}}\right)_6 \sqrt{gRT_6} \qquad (12)$$

where $\left(\frac{V}{\sqrt{gRT}}\right)_6$ was obtained from the charts of reference 8 and the static-pressure parameter $\left(\frac{pA}{W\sqrt{(R/g)T}}\right)_6$ as computed for the afterburner-inlet station with the assumption that $T_5 = T_6$.

REFERENCES

1. Wood, Charles C., Higginbotham, James T.: Performance Characteristics of a 24° Straight-Outer-Wall Annular-Diffuser-Tailpipe Combination Utilizing Rectangular Vortex Generators for Flow Control. NACA RM L53H17a, 1953.

2. Mallett, William E., and Harp, James L., Jr.: Performance Characteristics of Several Short Annular Diffusers for Turbojet Engine Afterburners. NACA RM E54B09, 1954.

3. Jansen, Emmert T., Jr., Velie, Wallace W., and Wilsted, H. Dean: Experimental Investigation of the Effect of Fuel-Injection-System Design Variables on Afterburner Performance. NACA RM E53K16, 1954.

4. Grey, Ralph E., Krull, H. G., and Sargent, A. F.: Altitude Investigation of 16 Flame-Holder and Fuel-System Configurations in Tail-Pipe Burner. NACA RM E51E03, 1951.

5. Fleming, W. A., Conrad, E. William, and Young, A. W.: Experimental Investigation of Tail-Pipe-Burner Design Variables. NACA RM E50K22, 1951.

6. Koffel, William K., and Kaufman, Harold R.: Investigation of Heat-Transfer Coefficients in an Afterburner. NACA RM E52D11, 1952.

7. Turner, L. Richard, and Bogart, Donald: Constant-Pressure Combustion Charts Including Effects of Diluent Addition. NACA Rep. 937, 1949. (Supersedes NACA TN's 1086 and 1655.)

8. Turner, L. Richard, Addie, Albert N., and Zimmerman, Richard H.: Charts for the Analysis of One-Dimensional Steady Compressible Flow. NACA TN 1419, 1948.

9. Sivo, Joseph N., and Fenn, David B.: A Method of Measuring Jet Thrust of Turbojet Engines in Flight Installations. NACA RM E53J15, 1954.

10. Grey, Ralph E., Jr., and Wilsted, H. Dean: Performance of Conical Jet Nozzles in Terms of Flow and Velocity Coefficients. NACA Rep. 933, 1949. (Supersedes NACA TN 1757.)

[redacted]

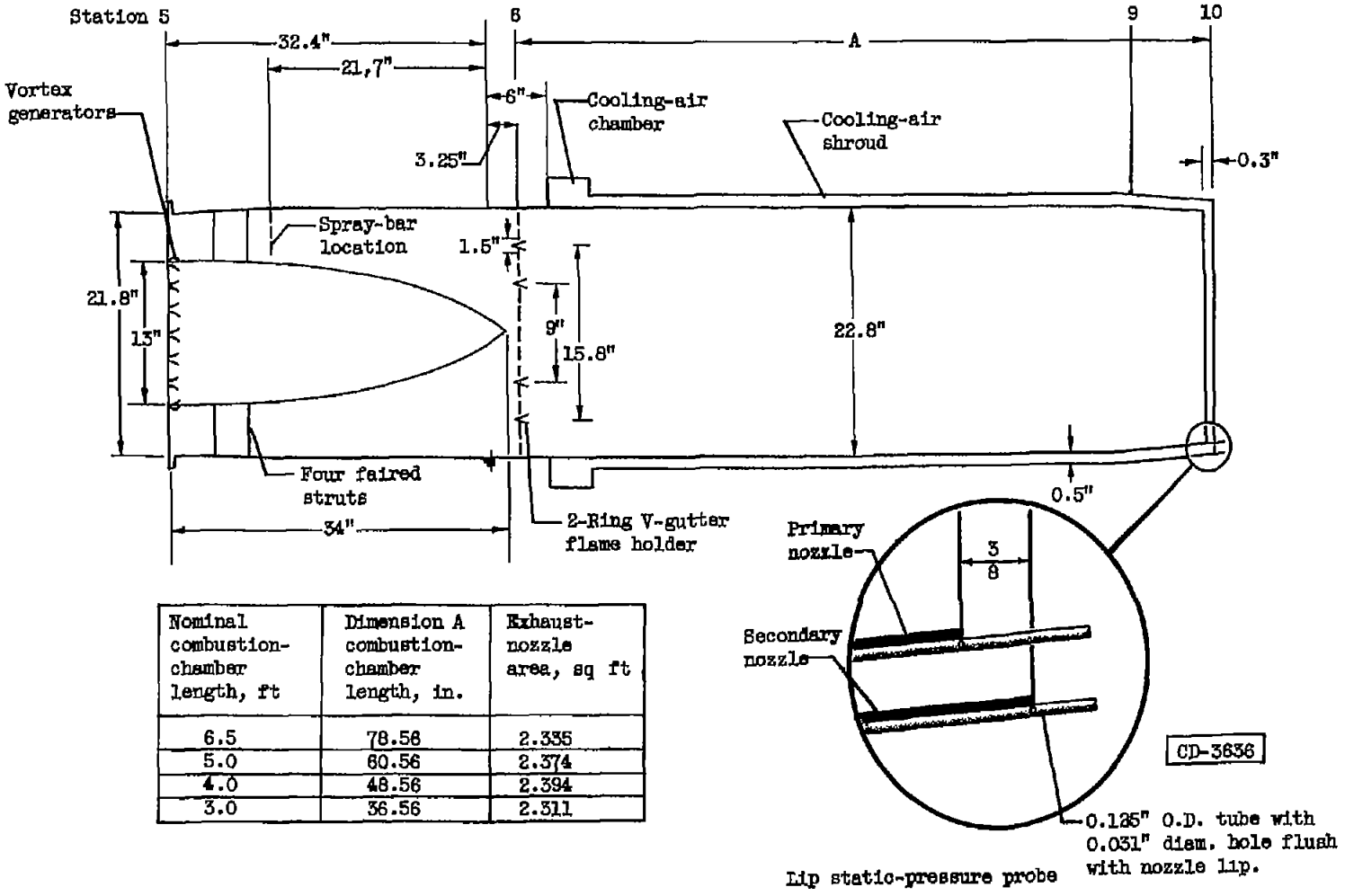

Nominal combustion-chamber length, ft	Dimension A combustion-chamber length, in.	Exhaust-nozzle area, sq ft
6.5	78.56	2.335
5.0	60.56	2.374
4.0	48.56	2.394
3.0	36.56	2.311

Figure 1. - Schematic diagram of afterburner with variable-length combustion chamber.

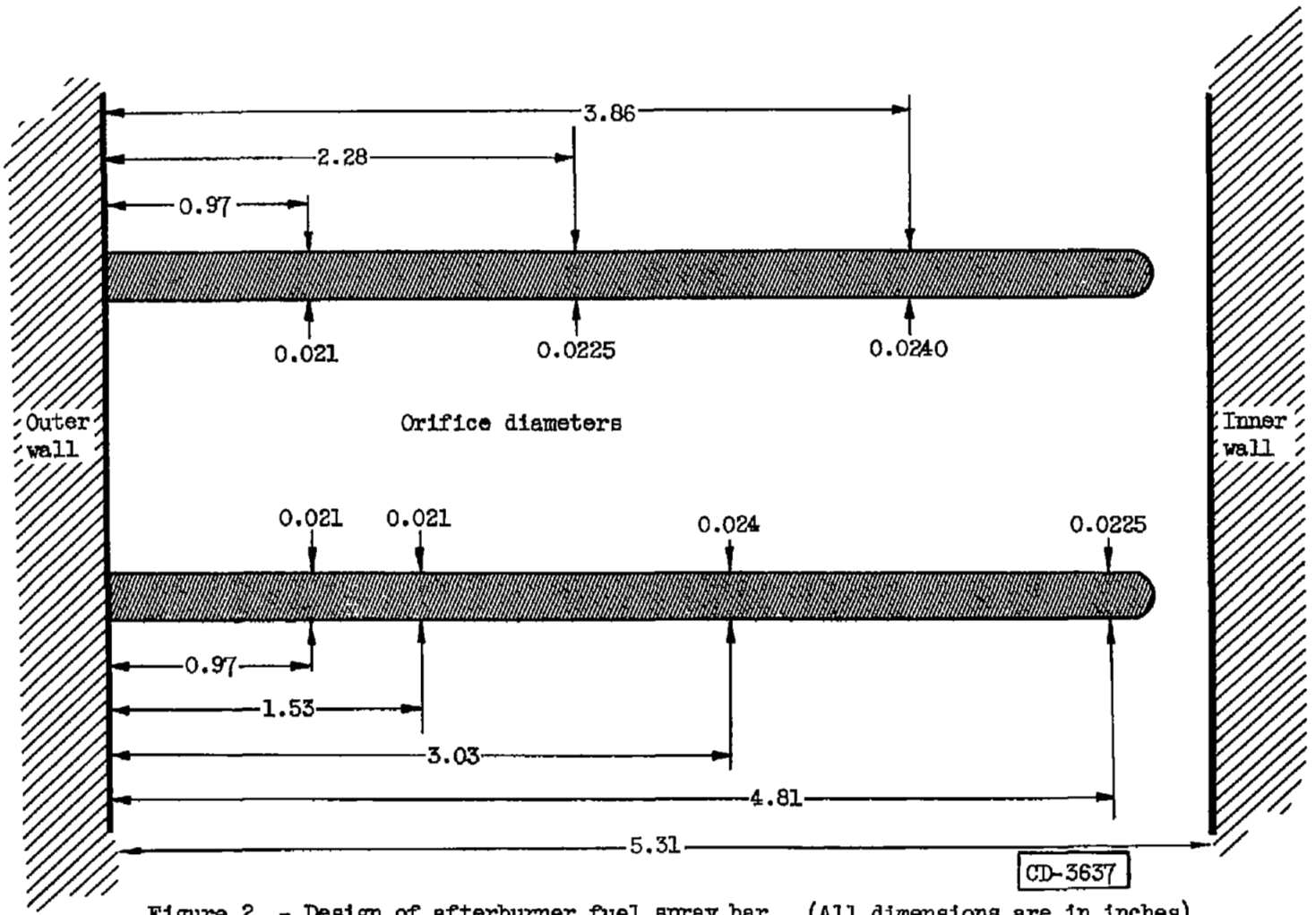

Figure 2. - Design of afterburner fuel spray bar. (All dimensions are in inches)

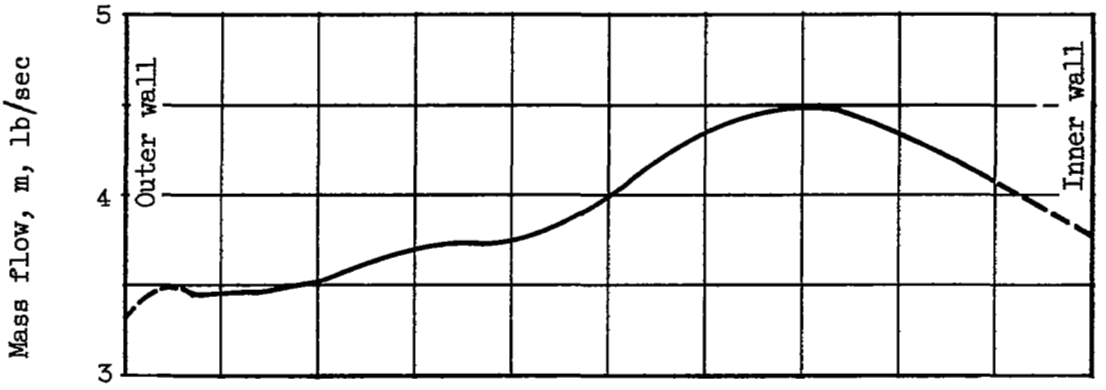

(a) Mass-flow profile at fuel-spray-bar location.

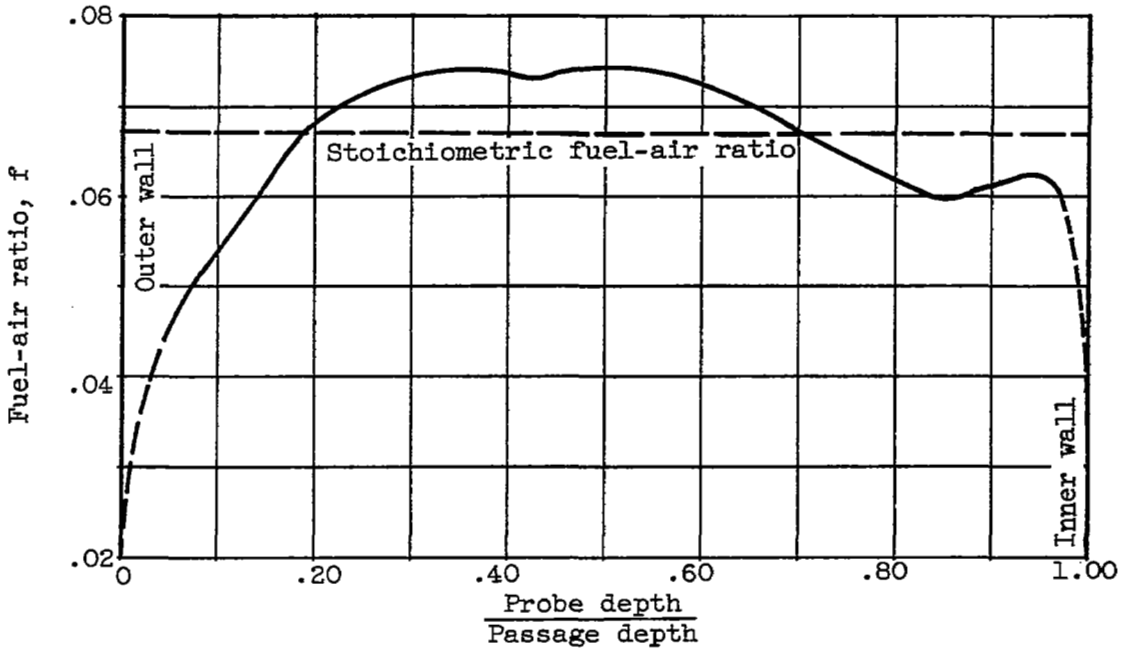

(b) Fuel-air ratio profile at flame holder.

Figure 3. - Typical mass-flow and fuel-air ratio profiles obtained during stoichiometric afterburning. Flight Mach number, 1.0; altitude, 35,000 feet; afterburner-inlet pressure, 1600 pounds per square foot absolute.

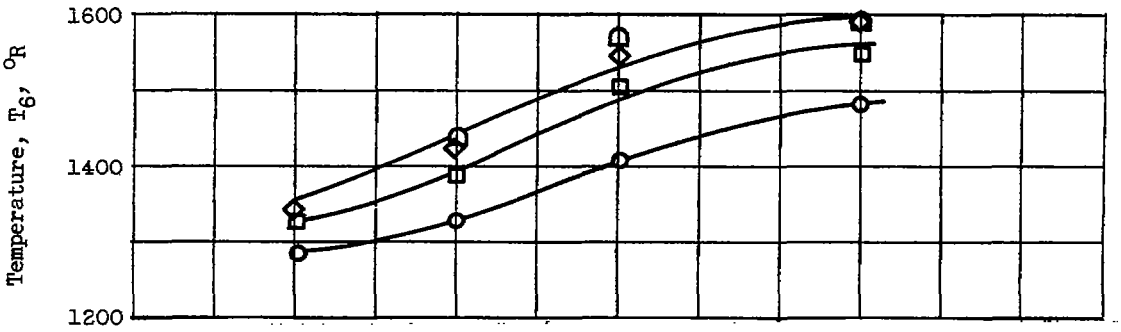

(a) Variation of afterburner-inlet temperature.

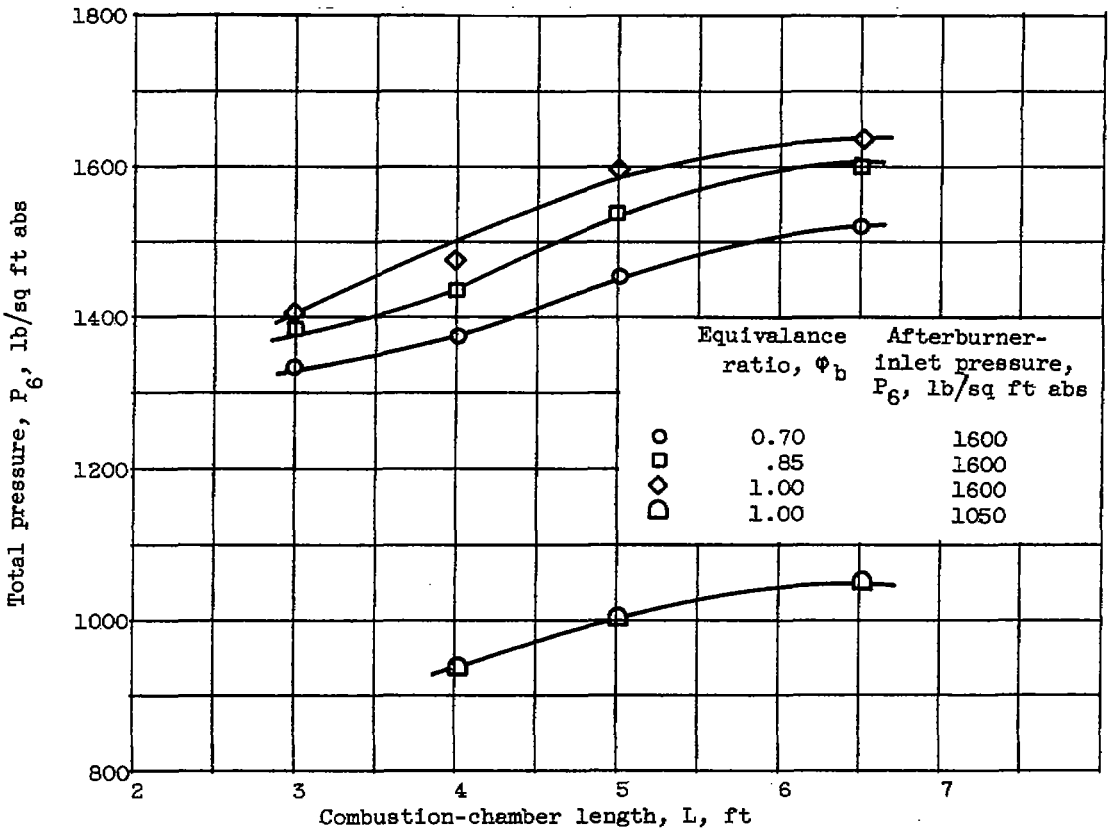

(b) Variation of afterburner-inlet total pressure.

Figure 4. - Variation of afterburner-inlet temperature, pressure, and velocity with combustion-chamber length.

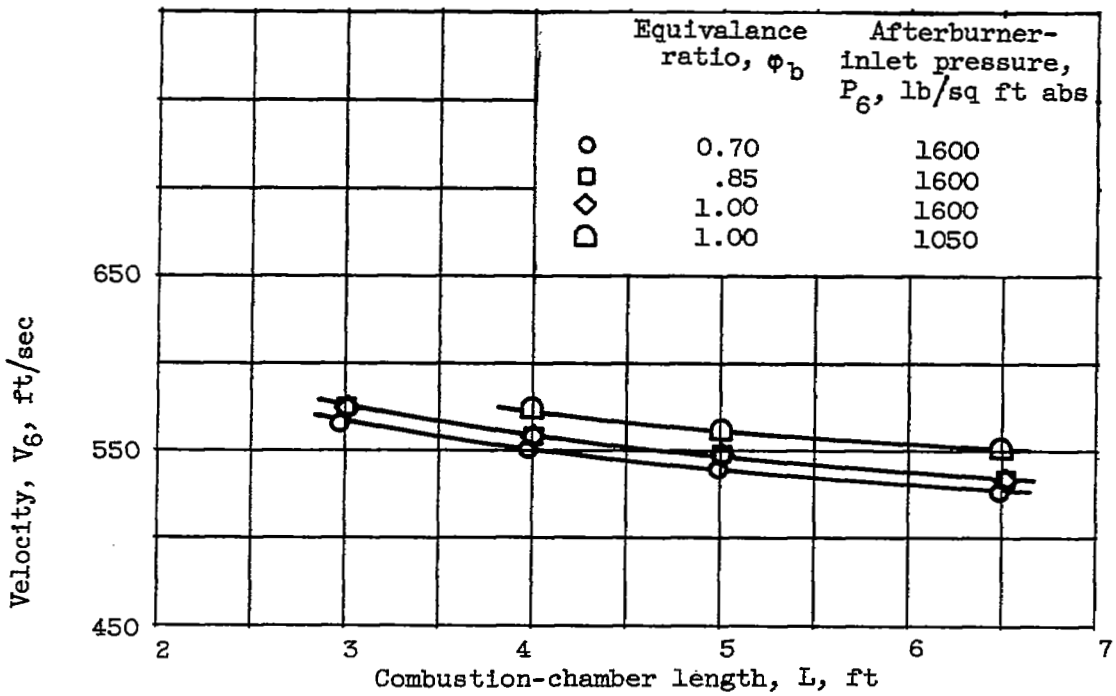

(c) Variation of afterburner-inlet velocity.

Figure 4. - Concluded. Variation of afterburner-inlet temperature, pressure, and velocity with combustion-chamber length.

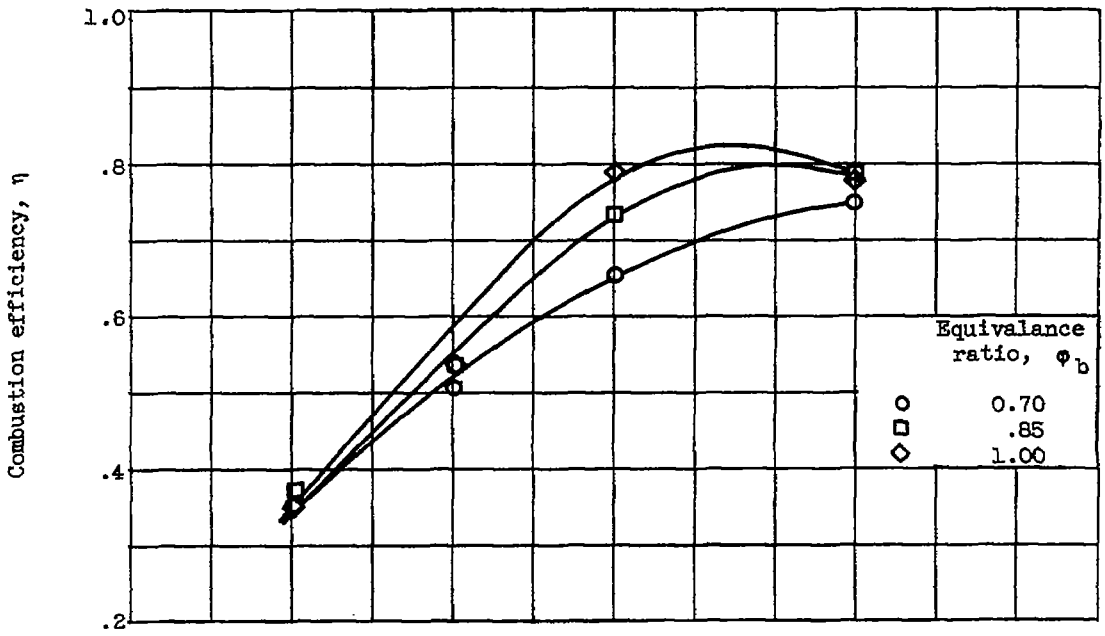

(a) Afterburner combustion efficiency.

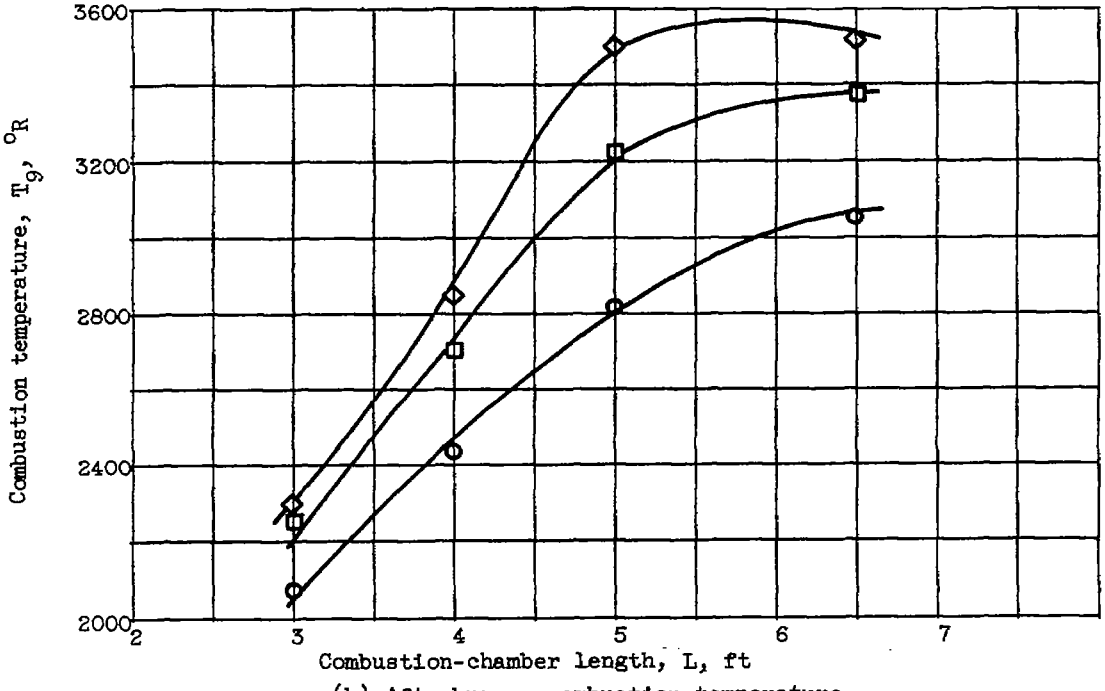

(b) Afterburner combustion temperature.

Figure 5. - Effect of combustion-chamber length on afterburner performance for several equivalance ratios. Flight Mach number, 1.0; altitude, 35,000 feet; afterburner-inlet pressure, 1600 pounds per square foot absolute.

[redacted]

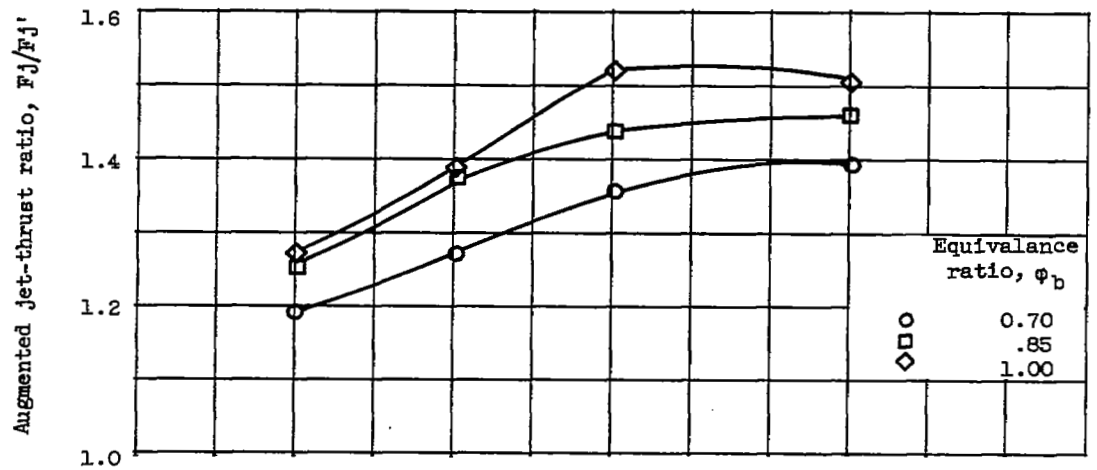

(c) Augmented jet-thrust ratio.

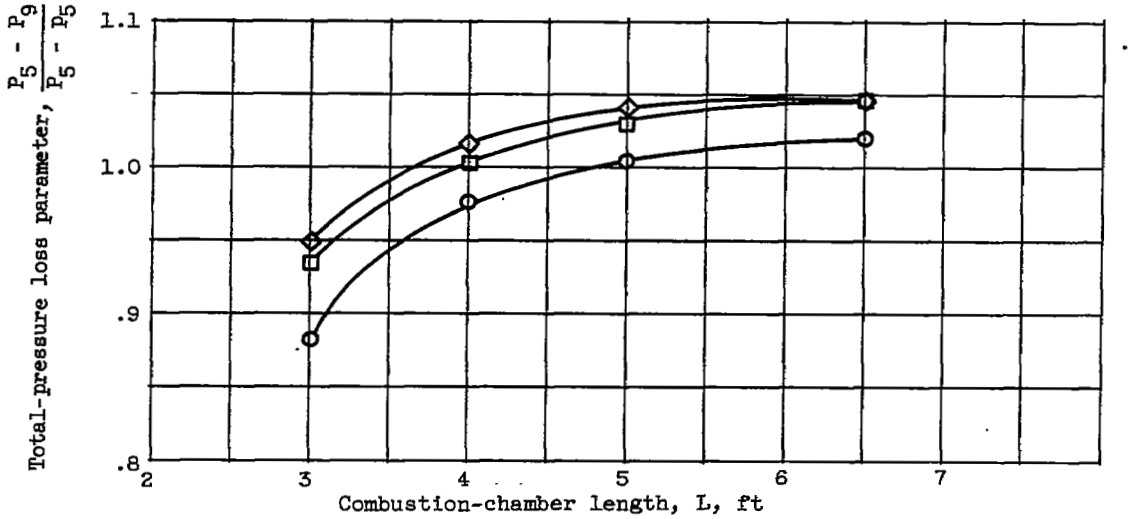

(d) Total-pressure loss parameters.

Figure 5. - Concluded. Effect of combustion-chamber length on afterburner performance for several equivalance ratios. Flight Mach number, 1.0; altitude, 35,000 feet; afterburner-inlet pressure, 1600 pounds per square foot absolute.

[redacted]

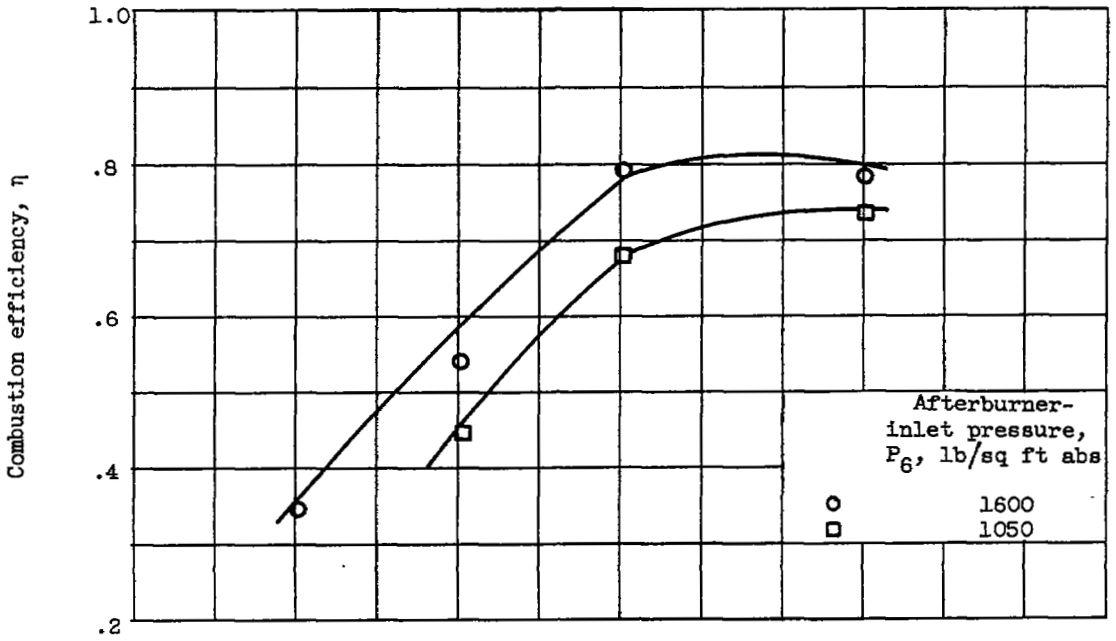

(a) Afterburner combustion efficiency.

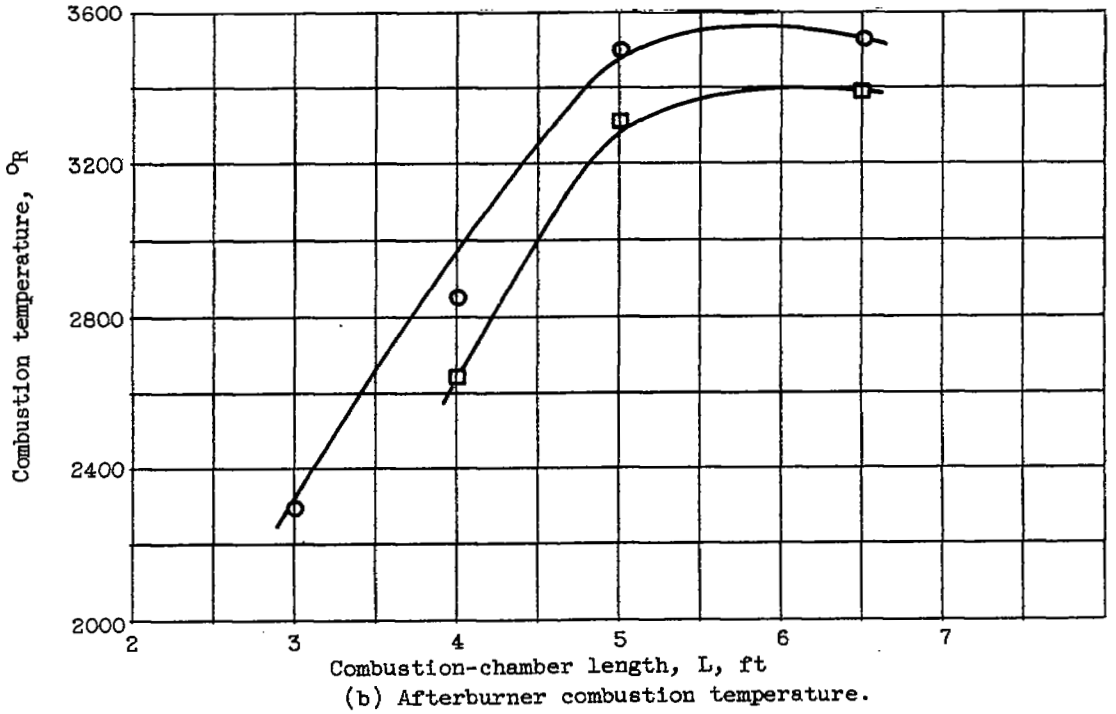

(b) Afterburner combustion temperature.

Figure 6. - Effect of variation in combustion-chamber length on afterburner performance for two flight conditions with stoichiometric afterburning.

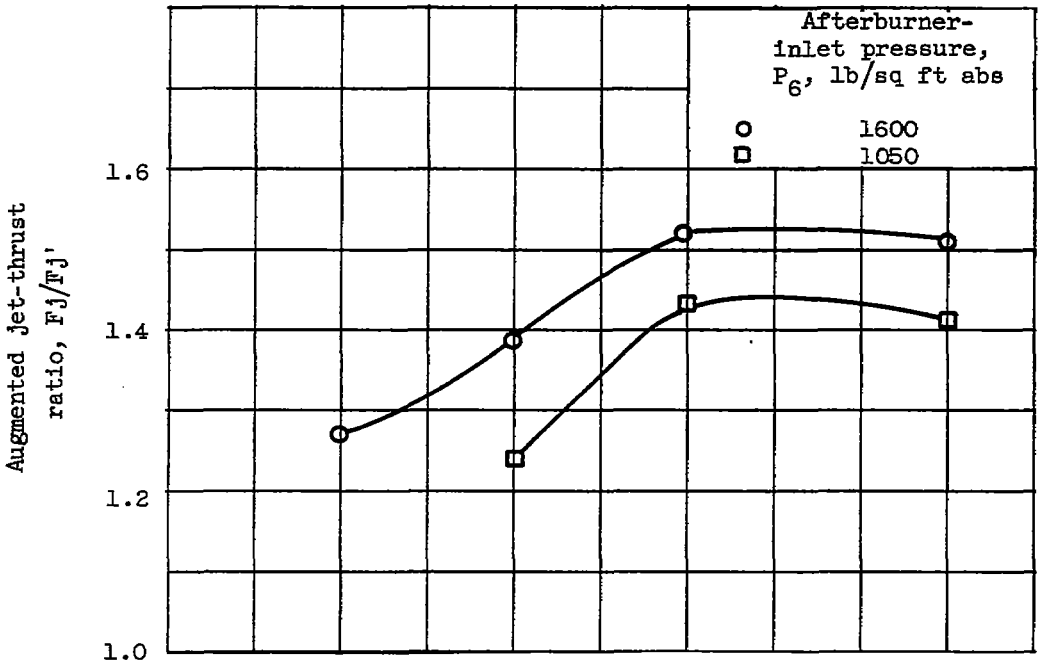

(c) Augmented jet-thrust ratio.

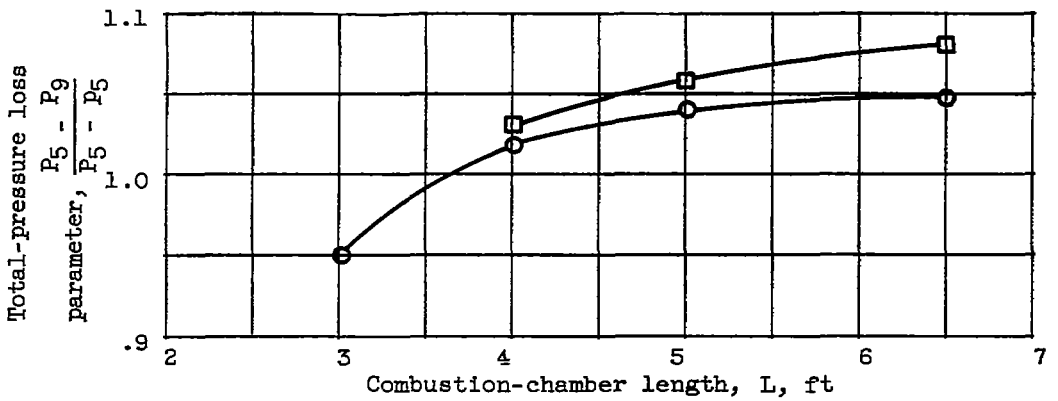

(d) Total-pressure loss parameter.

Figure 6. - Concluded. Effect of variation in combustion-chamber length on afterburner performance for two flight conditions with stoichiometric afterburning.

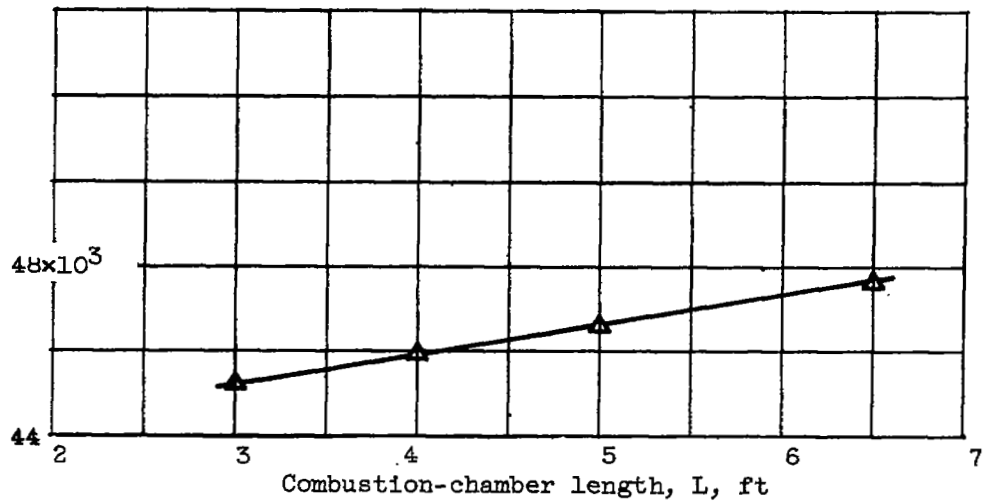

Figure 7. - Effect of combustion-chamber length on altitude operational limit. Flight Mach number, 0.8.

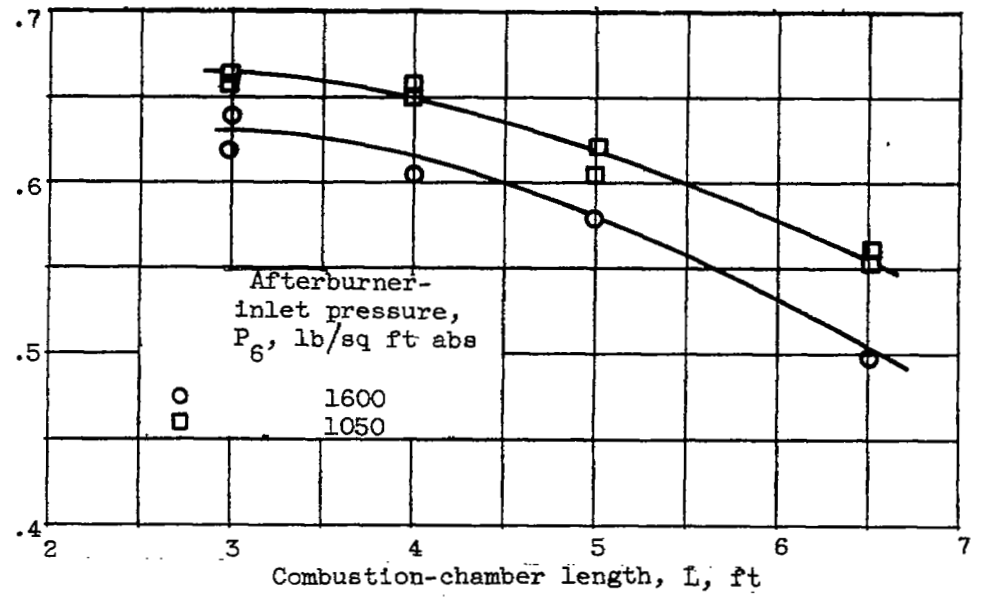

Figure 8. - Effect of combustion-chamber length on lean combustion blow-out operational limits.

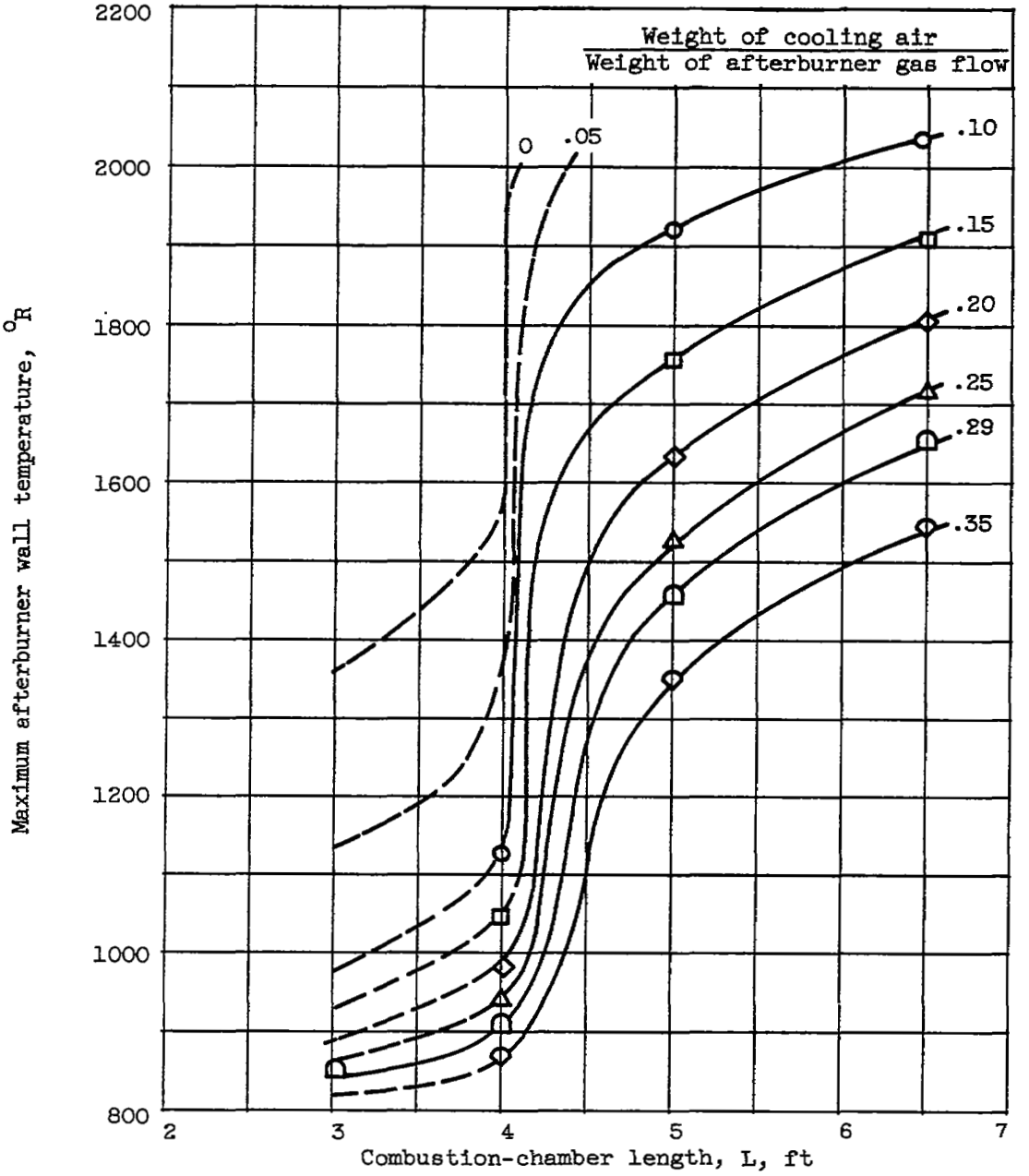

Figure 9. - Effect of afterburner combustion-chamber length on cooling of afterburner structure. Flight Mach number, 1.0; altitude, 35,000 feet; afterburner equivalance ratio, 1.0.